

This discussion paper is/has been under review for the journal Atmospheric Chemistry and Physics (ACP). Please refer to the corresponding final paper in ACP if available.

**Atmospheric
observation-based
global SF₆ emissions**

I. Levin et al.

Atmospheric observation-based global SF₆ emissions – comparison of top-down and bottom-up estimates

I. Levin¹, T. Naegler¹, R. Heinz¹, D. Osusko¹, E. Cuevas², A. Engel³,
J. Ilmberger¹, R. L. Langenfelds⁴, B. Neininger⁵, C. v. Rohden¹, L. P. Steele⁴,
R. Weller⁶, D. E. Worthy⁷, and S. A. Zimov⁸

¹Institut für Umweltphysik, University of Heidelberg, INF 229, 69120 Heidelberg, Germany

²Centro de Investigación Atmosférica de Izaña, Instituto Nacional de Meteorología (INM), C/La Marina, 20, Planta 6, 38071 Santa Cruz de Tenerife, Spain

³Institut für Atmosphäre und Umwelt, J. W. Goethe Universität Frankfurt, Altenhöferallee 1, 60438 Frankfurt/Main, Germany

⁴Centre for Australian Weather and Climate Research/CSIRO Marine and Atmospheric Research (CMAR), Private Bag No. 1, Aspendale, Victoria 3195, Australia

⁵MetAir AG, Flugplatz, 8915 Hausen am Albis, Switzerland

⁶Alfred Wegener Institute for Polar and Marine Research, Am Handelshafen 12, 27570 Bremerhaven, Germany

Title Page

Abstract

Introduction

Conclusions

References

Tables

Figures

◀

▶

◀

▶

Back

Close

Full Screen / Esc

Printer-friendly Version

Interactive Discussion



⁷Environment Canada, Climate Research Division/CCMR, 4905 Dufferin St., Toronto, ON M3H 5T4, Canada

⁸North East Section of the Russian Academy of Sciences, P.O. Box 18, Cherskii, Republic of Sakha (Yakutia), Russia

Received: 1 December 2009 – Accepted: 3 December 2009 – Published: 11 December 2009

Correspondence to: I. Levin (ingeborg.levin@iup.uni-heidelberg.de)

Published by Copernicus Publications on behalf of the European Geosciences Union.

ACPD

9, 26653–26672, 2009

**Atmospheric
observation-based
global SF₆ emissions**

I. Levin et al.

Title Page

Abstract

Introduction

Conclusions

References

Tables

Figures

⏪

⏩

◀

▶

Back

Close

Full Screen / Esc

Printer-friendly Version

Interactive Discussion



Abstract

Emissions of sulphur hexafluoride (SF_6), one of the strongest greenhouse gases on a per molecule basis, are targeted to be collectively reduced under the Kyoto Protocol. Because of its long atmospheric lifetime (≈ 3000 years), the accumulation of SF_6 in the atmosphere is a direct measure of its global emissions. Examination of our extended data set of globally distributed high-precision SF_6 observations shows an increase in SF_6 abundance from near zero in the 1970s to a global mean of 6.7 ppt by the end of 2008. In-depth evaluation of our long-term data records shows that the global source of SF_6 decreased after 1995, most likely due to SF_6 emission reductions in industrialised countries, but increased again after 1998. By subtracting those emissions reported by Annex I countries to the United Nations Framework Convention of Climatic Change (UNFCCC) from our observation-inferred SF_6 source leaves a surprisingly large gap of more than 70–80% of non-reported SF_6 emissions in the last decade.

1 Introduction

SF_6 is an extremely stable man-made gas, having a very high global warming potential. The industrial production of SF_6 began in 1953 for use as an insulation gas in high voltage facilities (Ko et al., 1993; Maiss and Brenninkmeijer, 1998). Anthropogenic emissions from the electricity sector (through leaks and intentional emissions from these installations) continue to form the largest source of SF_6 to the atmosphere, with additional contributions from magnesium production, semiconductor manufacturing as well as other minor sources (Olivier et al., 2005). SF_6 is primarily destroyed in the mesosphere; its atmospheric lifetime is estimated to range from 800 to 3200 yr (Ravishankara et al., 1993; Morris et al., 1995). Therefore, practically all SF_6 emitted to the atmosphere actually accumulates there, allowing us to directly infer its global emissions from the observed atmospheric concentration increase (Maiss and Levin, 1994). Assuming that the distribution of emissions is well known (e.g. from inventories

ACPD

9, 26653–26672, 2009

Atmospheric observation-based global SF_6 emissions

I. Levin et al.

Title Page

Abstract

Introduction

Conclusions

References

Tables

Figures

◀

▶

◀

▶

Back

Close

Full Screen / Esc

Printer-friendly Version

Interactive Discussion



such as EDGAR, 2009), SF₆ has been widely used as a tracer to compare and validate atmospheric transport models (e.g., Levin and Hesshaimer, 1996; Denning et al., 1999; Kjellström et al., 2000; Waugh and Hall, 2002; Peters et al., 2004; Gloor et al., 2007; Bönisch et al., 2008; Patra et al., 2009).

5 In this study, global SF₆ emissions from 1979 to 2008 are estimated using its recent accumulation rate in the atmosphere based on new observational data. These top-down source estimates, hereafter called *inferred emissions*, are compared to *global* annual emissions published in the most recent compilation of the EDGAR data base (EDGAR, 2009) which uses a so-called bottom-up approach, based on statistical information on the sources and their global distribution. Both, top-down inferred and bottom-up estimates are further compared to SF₆ emissions reported by Annex I countries to UNFCCC (2009). Annex I countries include all major industrial countries of Western Europe, Canada, the United States, Japan, Australia, and New Zealand, as well as Eastern European countries, the Russian Federation and Turkey. At least until the mid 1990s emissions from Annex I countries should comprise the major share of global SF₆ emissions. After 2000 emissions from newly industrialised countries also significantly contribute to the increasing global atmospheric SF₆ burden (EDGAR, 2009). The difficulties to validate, on the regional scale, reported bottom-up emissions with spatially distributed observations and atmospheric transport modelling will also be discussed.

2 The 30-yr atmospheric SF₆ record

Our SF₆ observational network data comprises: 1) long-term data records from Alert (Arctic), Izaña (sub-tropics, Tenerife Island), Cape Grim (Tasmania, Australia), and Neumayer (Antarctica), 2) two meridional profiles collected in November 1990 and November 1993 over the Atlantic Ocean (50° N to 68° S), 3) regular vertical aircraft profiles over the Rhine Valley (Germany), Syktyvkar (Russia), Cherskii (Siberia), and over Tasmania (Australia), and 4) stratospheric profiles collected between 1997 and

Atmospheric observation-based global SF₆ emissions

I. Levin et al.

Title Page

Abstract

Introduction

Conclusions

References

Tables

Figures

⏪

⏩

◀

▶

Back

Close

Full Screen / Esc

Printer-friendly Version

Interactive Discussion



**Atmospheric
observation-based
global SF₆ emissions**

I. Levin et al.

[Title Page](#)[Abstract](#)[Introduction](#)[Conclusions](#)[References](#)[Tables](#)[Figures](#)[⏪](#)[⏩](#)[◀](#)[▶](#)[Back](#)[Close](#)[Full Screen / Esc](#)[Printer-friendly Version](#)[Interactive Discussion](#)

2005 at Kiruna (Sweden), Aire sur l'Adour (France) and Teresina (Brazil). Details of the sampling techniques and site locations can be found in Maiss and Levin (1994), Langenfelds et al. (1996), Levin et al. (2001, 2002), Engel et al. (2002), Schmitgen et al. (2004), and Weller et al. (2006); they are summarized in Table 1. All samples have been analysed at the Institut für Umweltphysik, University of Heidelberg. A description of the analysis technique and the development of the Heidelberg SF₆ calibration scale is described by Maiss et al. (1996) as well as in the Supplementary Material Sects. 1 and 2 (<http://www.atmos-chem-phys-discuss.net/9/26653/2009/acpd-9-26653-2009-supplement.pdf>).

The tropospheric SF₆ records from Neumayer, Cape Grim, Izaña, Alert and the aircraft sites (altitude >2500 m) are displayed in Fig. 1. From 1998 to 2006 an almost constant increase rate (solid lines) is observed, suggesting near constant global SF₆ emissions; only in the last four years emissions are increasing again. The measurement records from Izaña and Alert, starting in 1991 and 1993, respectively, show that mixing ratios from the Northern Hemisphere are about 0.3 to 0.4 ppt higher than the Southern Hemispheric data from Cape Grim and Neumayer. The observed inter-hemispheric difference is due to the uneven distribution of sources (more than 95% of SF₆ emissions originate in the Northern Hemisphere, Olivier et al., 2005; EDGAR, 2009), combined with the ca. 1 yr interhemispheric exchange time of air masses.

3 A new top-down estimate of global SF₆ emissions

Observations at the four globally distributed stations and along meridional transects over the Atlantic Ocean show relatively uniform SF₆ mixing ratios north of 30° N, and south of about 15° S, connected by a nearly linear north-to-south decrease in the tropics (Maiss et al., 1996; Geller et al., 1997). If we assume that observations from these background stations and the Syktyvkar aircraft location represent the zonal mean tropospheric SF₆ mixing ratios in their respective latitudinal bands, it is possible to reconstruct the temporal evolution of the tropospheric SF₆ distribution from this network.

**Atmospheric
observation-based
global SF₆ emissions**

I. Levin et al.

Title Page

Abstract

Introduction

Conclusions

References

Tables

Figures

◀

▶

◀

▶

Back

Close

Full Screen / Esc

Printer-friendly Version

Interactive Discussion



Further, combination with observed stratospheric SF₆ profiles (Supplementary Fig. A2) yields an estimate of the temporal development of the global SF₆ distribution on a latitude – altitude grid, which – when integrated over the entire atmosphere – gives the temporal development of the global atmospheric SF₆ inventory (see Supplementary Material Sect. 3).

With an atmospheric lifetime of 800–3200 yr (Ravishankara et al., 1993; Morris et al., 1995), the total atmospheric SF₆ sink in 2005 was 0.04–0.17 Gg (1 Gg=10⁹ g), i.e. approximately 1–4% of the observed annual atmospheric increase of ca. 5–6 Gg. Considering that the oceanic sink is one order of magnitude smaller than the atmospheric sink (Ko et al., 1993), the total SF₆ sink can be neglected. Therefore, we claim that the first temporal derivative of the global atmospheric SF₆ inventory provides a direct observation-based estimate of global SF₆ emissions which are presented in Fig. 2a. Inferred global SF₆ emissions steadily increase from ca. 2.1±0.13 Gg/a in 1978 to 6.4±0.4 Gg/a in 1995 (Table 2). In 1996, just two years after the UNFCCC agreement went into force, global emissions start to drop and reach a minimum of 5.4±0.32 Gg/a in 1998; but they increase again to 6.8±0.4 Gg/a in 2007 and 2008. Our inferred annual emissions up to 2005 compare rather well (within a 2σ error margin of our estimates) with independent estimates from other observational studies (see Supplementary Fig. A3 and respective references in the Supplementary Material). Also the emissions estimated by EDGAR (2009) (Fig. 2a, solid black line) compare well with our data within ±20%, but it is not clear to us how independent the EDGAR (2009) emissions inventory is from observed atmospheric mixing ratio changes.

4 Comparison with data reported to UNFCCC

Figure 2a also shows the total share of annual SF₆ emissions which Annex I countries officially reported to UNFCCC (2009) from 1990 to 2006 (solid blue line). We applied a downward correction to the figure Japan reported to UNFCCC before 1994 (dashed blue line) because they probably overestimated pre-1994 emissions due to an inade-

quate methodology used (Jigme, UNFCCC, pers. comm., see Supplementary Material Sect. 4.2). While in 1990 total reported emissions by Annex I countries still correspond to 80% of the global inferred emissions, they decrease in 1995 to 43%, and to less than 24% in 2005. The EDGAR (2009) data base not only provides global emissions but also emissions per country. The annual sum of all Annex I emissions as estimated by EDGAR for 1976 to 2005 is also plotted in Fig. 2a (dashed-dotted black line). These emissions are higher by more than 90% compared to what was officially reported to UNFCCC for 1995, and by more than a factor of two from 1997 until 2005.

Newly industrialized countries not included in Annex I of the UNFCCC, such as China, India, Brazil, and others, are not required to report SF₆ emissions to UNFCCC. Their SF₆ emissions as estimated by EDGAR are displayed in Fig. 2b (dashed-dotted black line). These data are compared here with the residual emissions as calculated from the difference between the total observation-inferred SF₆ source and Annex I reported SF₆ emissions. These so-called non-reported emissions are also plotted in Fig. 2b, either based on originally reported or Japan-corrected emissions. We call these “scenarios” of SF₆ emissions “UNFCCC-based”. From 1995 to 2000 non-reported emissions in the UNFCCC-based scenario are more than three times higher than EDGAR estimates for Non-Annex I countries, and in 2000 they already account for about 2/3 of the global SF₆ source. Both, the *increase* of non-reported emissions and their respective *share* in the global emissions are surprisingly large, in particular if all these non-reported emissions would have to be assigned to emissions from Non-Annex I countries. The dominant sector for SF₆ use and emission is electricity production (Olivier and Berdowski, 2001). Interestingly, the share of Non-Annex I countries in global electricity production was only 1/3 in 2000 (BP, 2009). Assuming that the UNFCCC-based SF₆ emission scenario is correct therefore implies that the annual SF₆ emissions per GWh electricity production would be two to more than three times larger in Non-Annex I countries than in Annex I countries. The large discrepancies between the two emission scenarios, EDGAR and UNFCCC-based are further investigated in the next section.

**Atmospheric
observation-based
global SF₆ emissions**I. Levin et al.

[Title Page](#)[Abstract](#)[Introduction](#)[Conclusions](#)[References](#)[Tables](#)[Figures](#)[⏪](#)[⏩](#)[◀](#)[▶](#)[Back](#)[Close](#)[Full Screen / Esc](#)[Printer-friendly Version](#)[Interactive Discussion](#)

5 Comparison of observed mixing ratios with model simulations

A comparison of observed mixing ratios with atmospheric transport model estimates that are based on different emission scenarios may help to decide which of them is more likely correct. Here we have deployed the two emission distribution estimates, EDGAR and the corrected UNFCCC-based in a coarse-resolution two-dimensional atmospheric box model GRACE (Levin et al., 2009). Thereby, simulated tropospheric SF₆ mixing ratios were compared with observations at Alert (82° N), Cape Grim (41° S) and Neumayer (71° S). The core of the GRACE model consists of an atmospheric module with 28 boxes, representing zonal mean tracer mixing ratios in six zonal, and either four (tropics) or five (extra-tropics) vertical subdivisions. Air mass (and tracer) exchange between the atmospheric boxes is controlled by three processes: 1) (turbulent) diffusive exchange between neighbouring boxes, 2) the Brewer-Dobson circulation, and 3) seasonal lifting and lowering of the extra-tropical tropopause. While the meridional distribution of SF₆ emissions for the EDGAR scenario can be directly taken from the data base (EDGAR, 2009), we used for the source distribution of the UNFCCC-based scenario for Annex I countries the officially reported emissions corrected for Japan (UNFCCC, 2009). For Non-Annex I countries the residual from the global inferred SF₆ source (dotted blue line in Fig. 2b) was distributed according to the electrical power production of these countries (see Supplementary Material Sect. 4.3 and Fig. A4).

Simulated SF₆ mixing ratios from 1976 to 2009 for the mid latitude box of GRACE in the Southern Hemisphere are displayed in Fig. 3a, together with the observations at Cape Grim (41° S) starting in 1978. There is generally good agreement of the long-term trends between EDGAR-based simulations and the observations, with model results being slightly lower than observations up to 1992 and again from about 2003 onwards. When using the relative latitudinal distribution of SF₆ emissions from EDGAR adjusted to our observation-inferred annual totals, we obtain almost perfect agreement with observations for the whole period from 1978 until present. This confirms our top-down method, but also shows how sensitive global tropospheric SF₆ mixing ratio trends can

Atmospheric observation-based global SF₆ emissions

I. Levin et al.

Title Page

Abstract

Introduction

Conclusions

References

Tables

Figures

◀

▶

◀

▶

Back

Close

Full Screen / Esc

Printer-friendly Version

Interactive Discussion



reflect the underlying source strengths.

With the adjusted EDGAR distribution, the mixing ratios at Alert (82° N) and Neumayer (71° S) (inlay in Fig. 3a) as well as the north–south gradient (Fig. 3b, thick red line) are also correctly reproduced. However, model simulations using the UNFCCC-based emission scenario slightly underestimate the observed north-south gradient for the period of 1995 to the present (Fig. 3b, thick blue line). This could be an indication that in the UNFCCC-based scenario the distribution of sources is not correct, i.e. that emissions are overestimated in the Southern Hemisphere or in the tropics and underestimated in mid latitudes of the Northern Hemisphere. Except for Australia and New Zealand, inhabited regions of all Annex I countries are located in northern mid-latitudes (30° N–60° N), while large areas of Non-Annex I countries (i.e. Southern China, India and Brazil) are located in subtropical and tropical regions of the Northern and Southern Hemispheres. Consequently, a shift of SF₆ emissions from Annex I to Non-Annex I countries (e.g. after the beginning of the 1990s) would imply a southward redistribution of the global SF₆ source. This in turn should result in a smaller SF₆ mixing ratio difference between the north and the south, as simulated with the UNFCCC-based emission scenario after about 1992 (Fig. 3b).

Besides incorrect distribution of sources, model-data mismatch can, however, also be caused by several other factors: Meridional mixing in the model may be overestimated, resulting in under-estimation of inter-hemispheric SF₆ differences and vice versa. Also the observations at Alert and Neumayer may not necessarily be representative for the large GRACE model boxes. Atmospheric transport between the different boxes in GRACE, which was kept constant from year to year, has been optimized using bomb ¹⁴CO₂, ¹⁰Be/⁷Be, but also SF₆ with estimates of the total SF₆ source taken from Levin and Hesshaimer (1996), assumed to be spatially distributed according to the electricity production (Prather et al., 1987). However, this transport optimization still allows for an uncertainty of hemispheric residence times on the order of ±25%. Indeed, increasing hemispheric residence times by 25% would bring model simulations with the UNFCCC-based scenario almost into agreement with the observations (upper

**Atmospheric
observation-based
global SF₆ emissions**

I. Levin et al.

Title Page

Abstract

Introduction

Conclusions

References

Tables

Figures

◀

▶

◀

▶

Back

Close

Full Screen / Esc

Printer-friendly Version

Interactive Discussion



boundary of the blue hatched area in Fig. 3b); in this case the EDGAR distribution would over-estimate the north-south difference (upper boundary of the red hatched area in Fig. 3b). At this stage, using the observed north-south difference of SF₆ we thus cannot firmly reject one of the two SF₆ emission scenarios. This is mainly because of the lack of really independent validation of transport properties in our model, i.e. independent from any prior calibration with SF₆ or other tracers, whose emissions also have source distributions similar to that of electricity production, such as fluorocarbons (Prather et al., 1987). A possible tracer for transport validation may be ⁸⁵Krypton (Jacob et al., 1987; Levin and Hesshaimer, 1996) which is mainly emitted from nuclear fuel reprocessing plants. However, these ⁸⁵Krypton emissions are largely concentrated in a few large point sources (Winger et al., 2005), a distribution not suitable for transport validation of our coarse resolution GRACE model.

6 Conclusions

Rigorously assessing the reliability of the EDGAR or the UNFCCC-based emission *distribution*, and validation of reported emissions by Annex I countries, may perhaps, be possible with a high resolution atmospheric transport model; however, such a model needs to be very well validated to correctly simulate atmospheric transport and mixing. Also, this would require a denser observational network. At present we are thus left with only the evidence from total non-reported SF₆ emissions as well as from specific SF₆ emissions per electricity production, which suggests, that Annex I reported UNFCCC emissions during the 1990s (and possibly until today) may be too low. This suggestion is confirmed by the EDGAR (2009) data base which assumes similar emission factors for Annex I and Non-Annex I countries. It is likely for the last ten years that SF₆ leakage rates are larger e.g. in China and other Non-Annex I countries than in Annex I countries, but it seems implausible to assume that Non-Annex I SF₆ emissions per electricity production are 2 up to 4 times higher than for Annex I countries. Annex I reported emissions may be too low because of intrinsic uncertainties of estimated SF₆

Atmospheric observation-based global SF₆ emissions

I. Levin et al.

Title Page

Abstract

Introduction

Conclusions

References

Tables

Figures

◀

▶

◀

▶

Back

Close

Full Screen / Esc

Printer-friendly Version

Interactive Discussion



stored in end-use applications in the US and Europe (Maiss and Brenninkmeijer, 1998), and possibly due to underestimated emissions from economies in transition. The accelerating increase of *global* SF₆ emissions since the end of the 1990s may be linked to rising emissions from Non-Annex I countries, which *qualitatively* agree with their economic growth (e.g. China) (GDP, 2008). However, as long as these countries are not obliged to report their emissions to UNFCCC, there will remain large inaccuracies in related bottom-up emission estimates.

Our study clearly shows that top-down verification of reported emissions is without alternative for greenhouse gases budgeting. On a country level, such validation can, however, only be achieved with a dense network of high-precision atmospheric observations in combination with adequately calibrated atmospheric transport models. Top-down validation of *total global* SF₆ emissions is accurately possible *without* a sophisticated transport model, even with only one or a few globally distributed background stations. This mechanism should, therefore, be included as an additional measure in the Kyoto reporting process, as it provides the only and ultimate proof of total reported emissions (changes), at least for gases with well-known sinks such as SF₆, and other fluorinated and chlorinated compounds.

Acknowledgements. This work would not have been possible without the invaluable help from the technical personnel at the sampling sites, in particular, the late Laurie Porter at Cape Grim, Pedro Carretero at Izaña, the changing teams at the polar stations Alert and Neumayer as well as A. Varlagin at the Russian aircraft site. We wish to thank D. Wagenbach for many helpful discussions on the manuscript. This long-term work was partly funded by a number of agencies in Germany and Europe, namely the Ministry of Education and Science, Baden-Württemberg, Germany; the German Science Foundation, the German Minister of Environment; the German Minister of Science and Technology; the German Umweltbundesamt, and the European Commission, Brussels, as well as national funding agencies in Canada and Spain. Sampling at the Cape Grim Baseline Air Pollution Station has been supported by funding from the Australian Bureau of Meteorology. P. Fraser and P. Krummel of CMAR are acknowledged for their long-term support of the Cape Grim Air Archive program, and gathering the SF₆ inter-comparison results at Cape Grime (P.K.).

Atmospheric observation-based global SF₆ emissions

I. Levin et al.

[Title Page](#)[Abstract](#)[Introduction](#)[Conclusions](#)[References](#)[Tables](#)[Figures](#)[Back](#)[Close](#)[Full Screen / Esc](#)[Printer-friendly Version](#)[Interactive Discussion](#)

References

- British Petroleum Statistical Review of World Energy, available online at <http://www.bp.com/statisticalreview>, 2009.
- Bönisch, H., Hoor, P., Gurk, C., Feng, W., Chipperfield, M., Engel, A., and Bregman, B.: Model evaluation of CO₂ and SF₆ in the extratropical UT/LS region, *J. Geophys. Res.*, 113, D06101, doi:10.1029/2007JD008829., 2008
- Denning, A. S., Holzer, M., Gurney, K. R., Heimann, M., Law, R. M., Rayner, P. J., Fung, I. Y., Fan, S.-M., Taguchi, S., Friedlingstein, P., Balkanski, Y., Maiss, M., and Levin, I.: Three-dimensional transport and concentration of SF₆: a model intercomparison study (TransCom 2), *Tellus*, 51B, 266–297, 1999.
- EDGAR, Emission Database for Global Atmospheric Research (EDGAR): European Commission, Joint Research Centre (JRC)/Netherlands Environmental Assessment Agency (PBL), release version 4.0. <http://edgar.jrc.ec.europa.eu>, 2009.
- Engel, A., Strunk, M., Müller, M., Haase, H. P., Poss, C., Levin, I., and Schmidt, U.: Temporal development of total chlorine in the high latitude stratosphere based on reference distributions of mean age derived from CO₂ and SF₆, *J. Geophys. Res.*, 107(D12), 4136, doi:10.1029/2001JD000584, 2002.
- Geller, L. S., Elkins, J. W., Lobert, J. M., Clark, A. D., Hurst, D.F, Butler, J. H., and Myers, R. C.: Tropospheric SF₆: observed latitudinal distribution and trends, derived emissions and inter-hemispheric exchange time, *Geophys. Res. Lett.*, 24(6), 675–678, 1997.
- Gloor, M., Dlugokencky, E., Brenninkmeijer, C., Horowitz, L., Hurst, D. F., Dutton, G., Crevoisier, C., Machida, T., and Tans, P.: Three-dimensional SF₆ data and tropospheric transport simulations: signals, modeling accuracy, and implications for inverse modeling, *J. Geophys. Res.*, 112, D15112, doi:10.1029/2006JD007973, 2007.
- Jacob, D. J., Prather, M. J., Wofsy, S. C., and McElroy, M. B.: Atmospheric distribution of ⁸⁵Krypton simulated with a general circulation model, *J. Geophys. Res.*, 92(D6), 6614–6626, 1987.
- Kjellström, E., Feichter, J., and Hoffmann, G.: Transport of SF₆ and ¹⁴CO₂ in the atmospheric general circulation model ECHAM4, *Tellus*, 52B, 1–18, 2000.
- Ko, M. K. W., Sze, N. D., Wang, W. C., Shia, G., Goldman, A., Murkay, F. J., Murkay, D. G., and Rinsland, C. P.: Atmospheric sulphur hexafluoride: sources, sinks and greenhouse warming, *J. Geophys. Res.*, 98, 10499–10507, 1993.

Atmospheric observation-based global SF₆ emissions

I. Levin et al.

Title Page

Abstract

Introduction

Conclusions

References

Tables

Figures

◀

▶

◀

▶

Back

Close

Full Screen / Esc

Printer-friendly Version

Interactive Discussion



**Atmospheric
observation-based
global SF₆ emissions**

I. Levin et al.

Title Page

Abstract

Introduction

Conclusions

References

Tables

Figures

◀

▶

◀

▶

Back

Close

Full Screen / Esc

Printer-friendly Version

Interactive Discussion

Langenfelds, R. L., Fraser, P. J., Francey, R. J., Steele, L. P., Porter, L. W., and Allison, C. E.: The Cape Grim air archive: the first seventeen years, 1978–1995, in: Baseline Atmospheric Program (Australia) 1994–95, edited by: Francey, R. J., Dick, A. L., and Derek, N., Bureau of Meteorology and CSIRO Division of Atmospheric Research, Melbourne, Australia, 53–70, 1996.

Levin, I., Heinz, R., Walz, V., Langenfelds, R. L., Francey, R. J., Steele, L. P., and Spencer, D. A.: SF₆ from flask sampling, in: Baseline Atmospheric Program Australia 1997–98, edited by: Tindale, N. W., Derek, N., and Francey, R. J., Bureau of Meteorology and CSIRO Atmospheric Research, 87–88, Melbourne, Australia, 2001.

Levin, I., Ciais, P., Langenfelds, R., Schmidt, M., Ramonet, M., Gloor, M., Sidorov, K., Tchepakova, N., Heimann, M., Schulze, E. D., Vygodskaya, N. N., Shibistova, O., and Lloyd, J.: Three years of trace gas observations over the EuroSiberian domain derived from aircraft sampling – a concerted action, *Tellus*, 54B, 696–712, 2002.

Levin, I. and Hesshaimer, V.: Refining of atmospheric transport model entries by the globally observed passive tracer distributions of ⁸⁵Krypton and sulphur hexafluoride (SF₆), *J. Geophys. Res.*, 101(D11), 16745–16755, 1996.

Levin, I., Naegler, T., Kromer, B., Diehl, M., Francey, R. J., Gomez-Pelaez, A. J., Steele, L. P., Wagenbach, D., Weller, R., and Worthy, D. E.: Observations and modelling of the global distribution and long-term trend of atmospheric ¹⁴CO₂, *Tellus B*, doi:10.1111/j.1600-0889.2009.00446.x, in press, 2009.

Maiss, M. and Levin, I.: Global increase of SF₆ observed in the atmosphere, *Geophys. Res. Lett.*, 21, 569–572, 1994.

Maiss, M., Steele, L. P., Francey, R. J., Fraser, P. J., Langenfelds, R. L., Trivett, N. B. A., and Levin, I.: Sulfur hexafluoride – a powerful new atmospheric tracer, *Atmos. Environ.*, 30, 1621–1629, 1996.

Maiss, M. and Brenninkmeijer, C. A. M.: Atmospheric SF₆: trends, sources, and prospects, *Environ. Sci. Technol.*, 32, 3077–3086, 1998.

Morris, R. A., Miller, T. M., Viggiano, A. A., Paulson, J. F., Solomon, S., and Reid, G.: Effects of electron and ion reactions on atmospheric lifetimes of fully fluorinated compounds, *J. Geophys. Res.*, 100, 1287–1294, 1995.

Nakazawa, T., Shizawa, M., Higuchi, K., and Trivett, N. B. A.: Two curve fitting methods applied to CO₂ flask data, *Environmetrics*, 8, 197–218, 1997.

Olivier, J. G. J. and Berdowski, J. J. M.: Global emissions sources and sinks, in: *The Climate*



System, edited by: Berdowski, J., Guicherit, R., and Heij, B. J., A. A. Balkema Publishers/Swets & Zeitlinger Publishers, Lisse, The Netherlands, ISBN 90 5809 255 0, 33–78, 2001.

Olivier, J. G. J., Van Aardenne, J. A., Dentener, F., Ganzeveld, L., and Peters, J. A. H. W.: Recent trends in global greenhouse gas emissions: regional trends and spatial distribution of key sources, in: Non-CO₂ Greenhouse Gases (NCGG-4), edited by: v. Amstel, A., Millpress, Rotterdam, ISBN 90 5966 043 9, 325–330, 2005.

Patra, P. K., Takigawa, M., Dutton, G. S., Uhse, K., Ishijima, K., Lintner, B. R., Miyazaki, K., and Elkins, J. W.: Transport mechanisms for synoptic, seasonal and interannual SF₆ variations and “age” of air in troposphere, *Atmos. Chem. Phys.*, 9, 1209–1225, 2009, <http://www.atmos-chem-phys.net/9/1209/2009/>.

Peters, W., Krol, M. C., Dlugokencky, E. J., Dentener, F. J., Bergamaschi, P., Dutton, G., Velthoven, P. v., Miller, J. B., Bruhwiler, L., and Tans, P. P.: Toward regional-scale modeling using the two-way nested global model TM5: Characterization of transport using SF₆, *J. Geophys. Res.*, 109, D19314, doi:10.1029/2004JD005020, 2004.

Prather, M., McElroy, M., Wofsy, S., Russel, G., and Rind, D.: Chemistry of the global troposphere, Fluorocarbons as tracers of air motion, *J. Geophys. Res.*, 92, 6579–6613, 1987.

Ravishankara, A. R., Solomon, S., Turnipseed, A. A., and Warren, R. F.: The atmospheric lifetimes of long-lived halogenated species, *Science*, 259, 194–199, 1993.

Real Historical Gross Domestic Product (GDP) and Growth Rates of GDP for Baseline Countries/Regions (in billions of 2000 dollars) 1969–2007, Source: World Bank World Development Indicators, adjusted to 2000 base and estimated and projected values developed by the Economic Research Service, data available from <http://web.worldbank.org>, 2009.

Schmitgen, S., Ciais, P., Geiss, H., Kley, D., Volz-Thomas, A., Neininger, B., Baeumle, M., and Brunet, Y.: Carbon dioxide uptake of a forested region in southwest France derived from airborne CO₂ and CO measurements in a quasi-Lagrangian experiment, *J. Geophys. Res.*, 109(D14), D14302, doi:10.1029/2003JD004335, 2004.

UNFCCC: National greenhouse gas inventory data for the period 1995–2006, Secretariat of the United Nation Framework Convention on Climate Change, Bonn, Germany, data available online at http://unfccc.int/ghg_data/items/4133.php, 2009.

Waugh, D. W. and Hall, T. M.: Age of stratospheric air: theory, observations and models, *Rev. Geophys.*, 40, 1–10, 2002.

Weller, R., Levin, I., Wagenbach, D., and Minikin, A.: The air chemistry observatory at Neu-

**Atmospheric
observation-based
global SF₆ emissions**

I. Levin et al.

Title Page

Abstract

Introduction

Conclusions

References

Tables

Figures

◀

▶

◀

▶

Back

Close

Full Screen / Esc

Printer-friendly Version

Interactive Discussion



mayer Stations (GvN and NM-II) Antarctica, Polarforschung, 76(1–2), 39–46, 2007.
Winger, K., Feichter, J., Kalinowski, M. B., Sartorius, H., and Schlosser, C.: A new compilation of the atmospheric ⁸⁵Krypton inventories from 1945 to 2000 and its evaluation in a global transport model, J. Environ. Radioactiv., 80, 183–215, 2005

ACPD

9, 26653–26672, 2009

**Atmospheric
observation-based
global SF₆ emissions**

I. Levin et al.

Title Page

Abstract

Introduction

Conclusions

References

Tables

Figures

◀

▶

◀

▶

Back

Close

Full Screen / Esc

Printer-friendly Version

Interactive Discussion

26667



Table 1. Characteristics of SF₆ measurement stations; the column “type” distinguishes between long-term background stations (LTB), regular aircraft sampling (RAS) and balloon sites (B). For the balloon sites, the figure in brackets after the “B” denotes the number of vertical SF₆ profiles taken.

Station	Latitude	Longitude	Altitude (m a.s.l.)	Type	Sample type	Period
Alert (Canada)	82° 27′ N	62° 31′ W	50	LTB	High pressure cylinder	Apr 1993–Dec 2003
Alert (Canada)	82° 27′ N	62° 31′ W	50	LTB	Glass flask	Oct 2004–Apr 2009
Cherskii (Siberia, Russia)	68° 44′ N	161° 19′ E	150–3050	RAS	Glass flask	Sep 2003–Sep 2005
Kiruna (Sweden)	67° 51′ N	20° 13′ E	9500–30 400	B (6)	Cryosampler	Feb 1997–Jun 2003
Syktvykar (Russia)	61° 24′ N	52° 18′ E	200–3300	RAS	Glass flask	Jun 1998–Aug 2005
Rhine Valley (Germany)	47° 55′ N	7° 55′ E	270–3200	RAS	Glass flask	Nov 2001–Jun 2005
Aire sur l’Adour (France)	42° 42′ N	0° 16′ W	10 500–32 400	B (5)	Cryosampler	Dec 1994–Oct 2002
Izaña (Tenerife, Spain)	28° 18′ N	16° 29′ W	2400	LTB	High pressure cylinder	Jun 1991–Apr 1999
Teresina (Brazil)	5° 05′ S	42° 47′ W	15 200–34 300	B (2)	Cryosampler	Jun 2005
Cape Grim (Tasmania, Australia)	40° 41′ S	144° 41′ E	104	LTB	High pressure cylinder archive	Apr 1978–Oct 1994
Cape Grim (Tasmania, Australia)	40° 41′ S	144° 41′ E	164	LTB	Stainless steel flask	Jan 1996–Jun 2009
Cape Grim (Tasmania, Australia)	40° 41′ S	144° 41′ E	300–7600	RAS	Glass flask	Feb 1997–Dec 1999
Neumayer (Antarctica)	70° 39′ S	8° 15′ E	30	LTB	High pressure cylinder	Aug 1986–Jan 2008
Neumayer (Antarctica)	70° 39′ S	8° 15′ E	30	LTB	Glass flask	Mar 1994–Jan 2009

Atmospheric observation-based global SF₆ emissions

I. Levin et al.

Title Page

Abstract

Introduction

Conclusions

References

Tables

Figures

◀

▶

◀

▶

Back

Close

Full Screen / Esc

Printer-friendly Version

Interactive Discussion



Table 2. Observed global atmospheric SF₆ inventory and inferred annual SF₆ source. The 1 σ uncertainties of the inventory are ± 3 –4 Gg, while the uncertainties of the annual emissions are $\pm 6\%$, neglecting oceanic and atmospheric sinks. Note that the inventory refers to the middle of each year, whereas the source refers to the period 1 January–31 December.

Year	Global inventory (Gg)	Global annual source (Gg)
1978	15.93	2.07
1979	17.81	2.25
1980	20.17	2.52
1981	22.85	2.84
1982	25.79	3.05
1983	28.92	3.21
1984	32.24	3.48
1985	35.91	3.89
1986	40.00	4.28
1987	44.36	4.39
1988	48.70	4.30
1989	53.00	4.32
1990	57.52	4.77
1991	62.45	5.14
1992	67.79	5.57
1993	73.57	6.00
1994	79.75	6.36
1995	86.17	6.41
1996	92.44	6.04
1997	98.24	5.56
1998	103.68	5.35
1999	109.01	5.42
2000	114.53	5.53
2001	120.04	5.51
2002	125.59	5.63
2003	131.31	5.79
2004	137.12	5.84
2005	143.01	5.98
2006	149.12	6.29
2007	155.63	6.79
2008	162.63	6.80

**Atmospheric
observation-based
global SF₆ emissions**

I. Levin et al.

Title Page

Abstract

Introduction

Conclusions

References

Tables

Figures

◀

▶

◀

▶

Back

Close

Full Screen / Esc

Printer-friendly Version

Interactive Discussion



Atmospheric observation-based global SF₆ emissions

I. Levin et al.

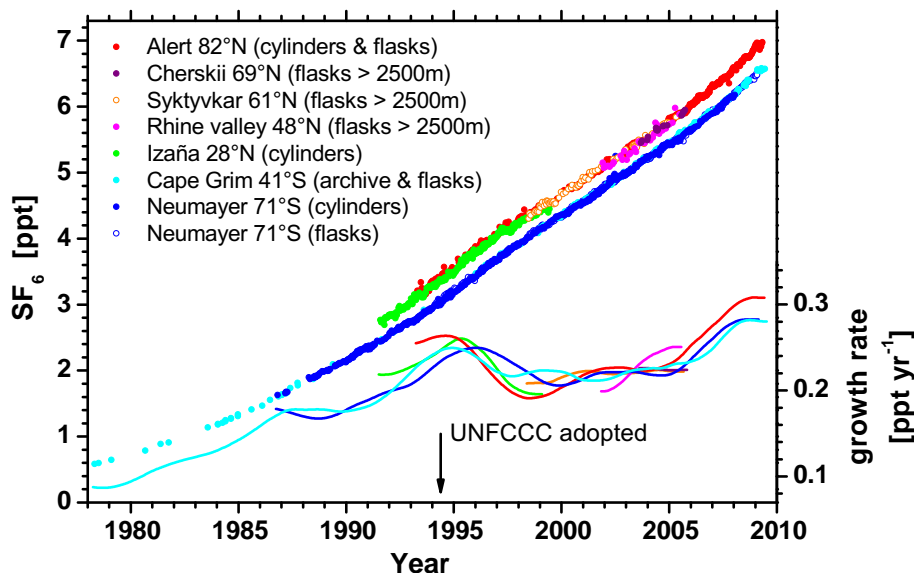


Fig. 1. Global observations of tropospheric SF₆. Symbols and left axis: atmospheric SF₆ mixing ratios (given in ppt=parts per trillion, i.e. picomoles of SF₆ per mole of dry air) observed in the Northern and Southern Hemispheres. The overlapping flask and cylinder data from Neumayer are virtually indistinguishable (note that 12 data points in total have been rejected as outliers from the Figure). Lines and right axis: SF₆ growth rates calculated for individual stations from de-seasonalized measurements using a fit routine from Nakazawa et al. (1997) (colour codes: same as original data).

[Title Page](#)
[Abstract](#)
[Introduction](#)
[Conclusions](#)
[References](#)
[Tables](#)
[Figures](#)
[◀](#)
[▶](#)
[◀](#)
[▶](#)
[Back](#)
[Close](#)
[Full Screen / Esc](#)
[Printer-friendly Version](#)
[Interactive Discussion](#)


Atmospheric
observation-based
global SF₆ emissions

I. Levin et al.

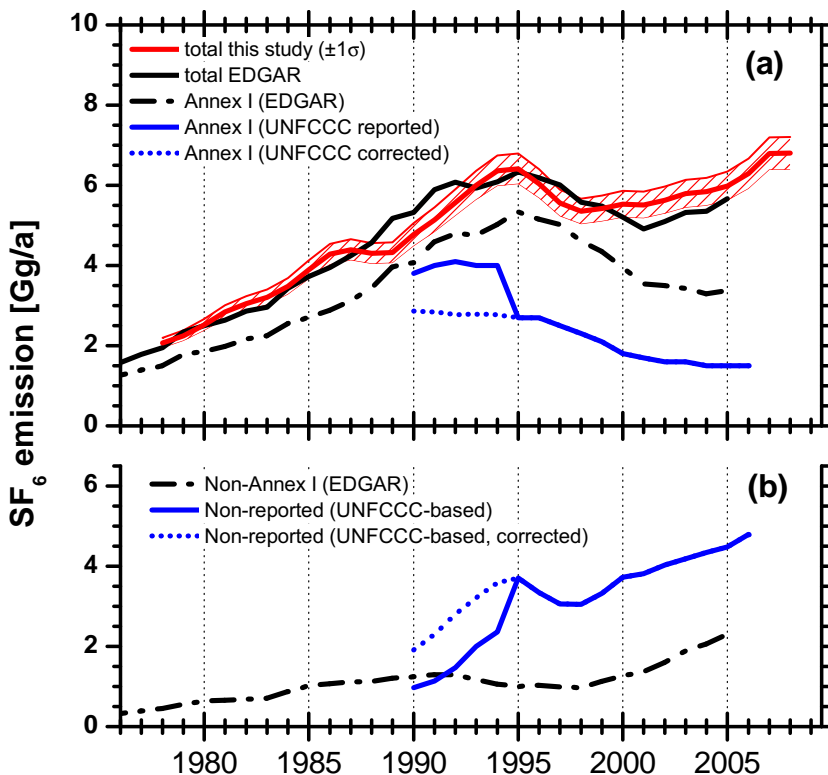


Fig. 2. (a) Comparison of annual observation-inferred global SF₆ emissions (red line with $\pm 1\sigma$ uncertainty range) with global emissions estimated by EDGAR (2009). Also included are the (Japan-corrected and original, see main text) emissions reported by Annex I countries to UNFCCC in 2009 (dashed resp. solid blue line) as well as estimated Annex I emissions from the EDGAR data base. (b) SF₆ emissions for Non-Annex I countries from the EDGAR data base (dashed dotted line) as well as non-reported emissions, calculated as residual from the total inferred source in (a) and UNFCCC-reported Annex I emissions (blue lines).

[Title Page](#)[Abstract](#)[Introduction](#)[Conclusions](#)[References](#)[Tables](#)[Figures](#)[◀](#)[▶](#)[◀](#)[▶](#)[Back](#)[Close](#)[Full Screen / Esc](#)[Printer-friendly Version](#)[Interactive Discussion](#)

Atmospheric observation-based global SF₆ emissions

I. Levin et al.

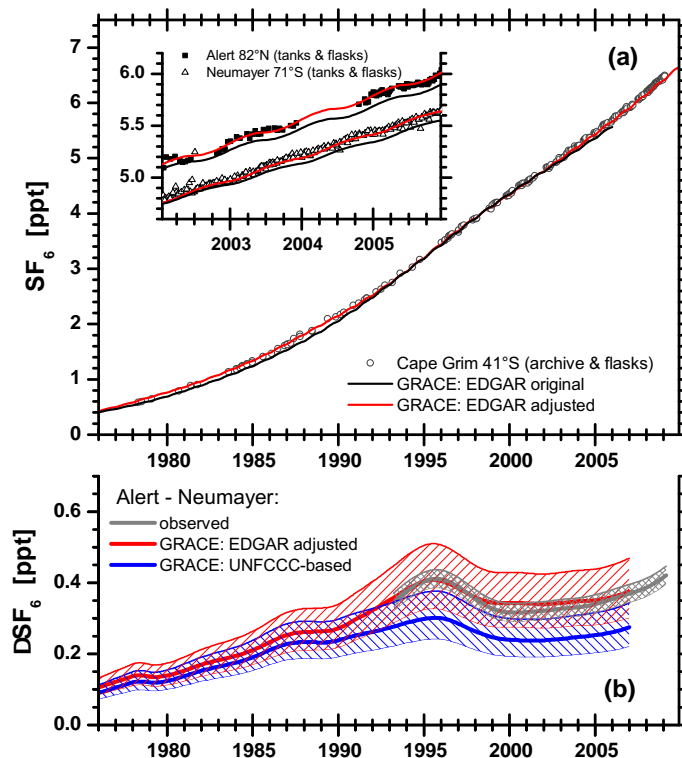


Fig. 3. Comparison of observed and simulated SF₆ mixing ratios and north-south differences: **(a)** SF₆ observations from Cape Grim (41° S), Alert (82° N) and Neumayer (71° S) (inlay) in comparison with GRACE simulations for the respective model box, based on the original EDGAR (2009) emissions (black lines) as well as simulations obtained when total EDGAR emissions were adjusted to the inferred emissions from Fig. 2a (red line). **(b)** SF₆ differences between Alert and Neumayer (taken from the fitted curves through the data and 1σ error estimates, grey line and hatched area) in comparison with GRACE simulations. Hatched areas show model results when inter-hemispheric transport is varied by ±25%.

Title Page

Abstract

Introduction

Conclusions

References

Tables

Figures

◀

▶

◀

▶

Back

Close

Full Screen / Esc

Printer-friendly Version

Interactive Discussion

